Biophysical Journal
Article

Biophysical Society

# Hypotonic Challenge of Endothelial Cells Increases Membrane Stiffness with No Effect on Tether Force

Manuela Aseye Ayele Ayee,[1] Elizabeth LeMaster,[1] Tao Teng,[2] James Lee,[2] and Irena Levitan[1,*]
[1]Division of Pulmonary, Critical Care, Sleep, and Allergy, Department of Medicine and [2]Department of Bioengineering, University of Illinois at Chicago, Chicago, Illinois

ABSTRACT Regulation of cell volume is a fundamental property of all mammalian cells. Multiple signaling pathways are known to be activated by cell swelling and to contribute to cell volume homeostasis. Although cell mechanics and membrane tension have been proposed to couple cell swelling to signaling pathways, the impact of swelling on cellular biomechanics and membrane tension have yet to be fully elucidated. In this study, we use atomic force microscopy under isotonic and hypotonic conditions to measure mechanical properties of endothelial membranes including membrane stiffness, which reflects the stiffness of the submembrane cytoskeleton complex, and the force required for membrane tether formation, reflecting membrane tension and membrane-cytoskeleton attachment. We find that hypotonic swelling results in significant stiffening of the endothelial membrane without a change in membrane tension/membrane-cytoskeleton attachment. Furthermore, depolymerization of F-actin, which, as expected, results in a dramatic decrease in the cellular elastic modulus of both the membrane and the deeper cytoskeleton, indicating a collapse of the cytoskeleton scaffold, does not abrogate swelling-induced stiffening of the membrane. Instead, this swelling-induced stiffening of the membrane is enhanced. We propose that the membrane stiffening should be attributed to an increase in hydrostatic pressure that results from an influx of solutes and water into the cells. Most importantly, our results suggest that increased hydrostatic pressure, rather than changes in membrane tension, could be responsible for activating volume-sensitive mechanisms in hypotonically swollen cells.

## INTRODUCTION

All cells maintain their volume within a narrow range to preserve normal cell function. The mechanisms of cell volume regulation have been an area of active investigation for several decades and multiple signaling pathways have been identified to be sensitive to cell swelling and to contribute to regulatory volume decrease (1,2). One important question that is still a matter of controversy is the impact of osmotic swelling on cellular biomechanics, which is proposed to play a key role in activating various mechanosensitive pathways.

Initially, it was proposed that cell swelling should result in an increase in membrane tension, which in turn should activate mechanosensitive ion channels leading to a reequilibration of the osmotic balance between the cytosol and the extracellular fluid, and thus, regulatory volume decrease. Moreover, osmotic challenge was used in a number of studies to determine whether specific processes were sensitive to changes in membrane tension (3–6), which was based on the assumption that cell swelling should necessarily lead to higher membrane tension. This assumption, however, may not be correct because of the highly folded nature of the plasma membranes of mammalian cells (7), which may lead to a significant increase in cell volume due to membrane unfolding without any increase in membrane tension. Indeed, the experimental data on membrane tension in cells under osmotic stress has been controversial: an earlier study of molluscan neurons found a significant increase in membrane tension during swelling, as estimated by pulling membrane tethers (3), whereas later studies of mammalian cells found no effect on tension unless membrane folds were flattened by genetic deficiency of Caveolin-1 or by cholesterol depletion (8). In both studies, membrane tension was estimated by measuring the force required to pull membrane tethers/nanotubes using optical tweezers, a method that measures an effective membrane tension, which depends on lipid bilayer tension per se and the adhesion energy between the submembrane cytoskeleton and the membrane bilayer (9,10). It is not possible to fully separate these parameters in a living cell without completely destroying the cytoskeleton or separating it from the membrane.

*Submitted September 8, 2017, and accepted for publication December 27, 2017.*

*Correspondence: levitan@uic.edu

Editor: Joseph Falke.
https://doi.org/10.1016/j.bpj.2017.12.032

Another important cellular biomechanical parameter is the elastic modulus, which is estimated by measuring the force required to induce a local deformation on the cell surface, and is typically obtained using atomic force microscopy (AFM) (11). Multiple studies have demonstrated that the membrane elastic modulus of living cells depends primarily on the submembrane cytoskeleton, which represents the mechanical scaffold of the cells (reviewed by (12,13)). Because cell swelling is expected to induce disruption of the cytoskeleton (14–21) and possibly its detachment from the membrane, cell swelling could be expected to result in cell softening as well. It is not clear, however, how the two biomechanical parameters (membrane tension and elastic modulus) are interrelated during cell swelling. In this study, therefore, we present a simultaneous analysis of the impact of osmotic swelling on endothelial elastic moduli, obtained by AFM nanoindentation, and on membrane tension, assessed by measuring membrane tether force in the same cells. We show that, in endothelial cells, swelling results in an increase in the elastic modulus of the membrane, which is paradoxically enhanced by the disruption of F-actin. Moreover, we find no effect of swelling on the force needed for membrane tether formation.

## MATERIALS AND METHODS

### Cell culture and reagents

Human aortic endothelial cells (HAECs; Lonza, Walkersville, MD) were grown between passages 6 and 13 and cultured according to the manufacturer's instructions in Lonza Clonetics Endothelial Growth Medium with EGM-2 BulletKit supplements. Gibco Penicillin-Streptomycin (Thermo Fisher Scientific, Waltham, MA) antibiotics were added to the medium at a concentration of 100 U/mL (penicillin) and 100 $\mu$g/mL (streptomycin) to prevent bacterial contamination. Cell cultures were maintained in a humidified incubator at 37°C with 5% $CO_2$ and were fed and split every 3–4 days.

### Cell treatments

HyClone Dulbecco's phosphate buffered saline (PBS) with calcium and magnesium was purchased from GE Healthcare (Logan, UT). HAECS were seeded on uncoated glass coverslips in six-well plates and grown in Lonza medium until confluent. The medium was removed and the HAECs were washed with PBS. Finally, to determine the effect of osmotic challenge on cell mechanics, HAECs were treated immediately before experiments with either PBS alone, with 20% hypotonic PBS, prepared by diluting PBS with cell culture grade distilled water, or with 20% hypertonic PBS, prepared by adding D-mannitol (Sigma-Aldrich, St. Louis, MO) to PBS. To disrupt the F-actin network, HAECs were treated with 1 $\mu$M latrunculin A (Cayman Chemical, Ann Arbor, MI) for 10 min, followed by changing medium to first isotonic PBS and then hypotonic PBS.

### Atomic force microscopy

The elastic modulus and force of membrane tether formation of individual HAECs was measured with an MFP-3D-BIO AFM (Oxford Instruments Asylum Research, Santa Barbara, CA). Briefly, cells were probed using gold-coated silicon nitride cantilevers with pyramidal tips (Cat. No. TR400PB, 2.9 $\mu$m height, 30 nm radius, 0.09 $\pm$ 0.06 N/m spring constant; Oxford Instruments Asylum Research). The cantilever was positioned above the cell between the nucleus and the cell edge, avoiding the perinuclear and edge regions, and each cell was probed in direct contact mode at two different locations, 25–50 times at each location. A total of 15–60 cells was analyzed for each experimental condition, with 50–100 force/distance curves acquired from each cell. The force curves were obtained by recording the force applied and the cantilever deflection at vertical $z$ positions of the cantilever as it approached, indented, and retracted from the cell. In some cases, adhesion occurred between the AFM cantilever tip and the cell membrane, resulting in sudden discontinuities in the retraction force curves as the membrane ruptured from the tip. The cantilever approached the cell at a velocity of 2 $\mu$m/s until a trigger force of 3 nN was reached, which corresponded to a 0.5 $\mu$m indentation depth. Before the start of each experiment, the cantilever is calibrated against a clean glass coverslip by calibrating the inverse optical lever sensitivity (InvOLS), a parameter that measures the photodiode response (in volts) per nanometer of cantilever deflection. The cantilever spring constant is then calibrated using a thermal-tune method during which the thermal vibrations of the cantilever are recorded and the power spectrum obtained is analyzed by the AFM software. We perform a fit to the lowest frequency thermal peak to obtain the cantilever spring constant. Finally, we perform a calibration of the InvOLS again on a section of glass that contains no cells when a sample is loaded, to obtain the cantilever sensitivity in the liquid medium environment. InvOLS is calibrated every time a cell sample is changed because the laser alignment may change.

### Measurement of cellular elastic moduli and membrane tether formation force

For each experiment, cells were first probed in AFM contact mode in an isotonic PBS solution. Then the same population of cells was probed after exchanging the isotonic solution with 20% hypotonic PBS. Each contact of the AFM tip with a cell resulted in both an approach (as the tip came closer to the surface of the cell) and a retraction (as the tip retreated from the cell surface after contact) force/distance curve, and both curves were analyzed to estimate cellular elastic moduli and membrane tether forces respectively (see representative force curves in Fig. 1, *A* and *B*).

To obtain Young's elastic moduli of the cells as a measure of cell stiffness, $E$, at least five force/distance approach curves at both locations probed on each cell were analyzed by fitting the experimental curve to the Hertz model for pyramidal tip geometries (22) (Eq. 1):

$$F = \frac{E \tan \phi}{2^{1/2}(1-\upsilon^2)}\delta^2, \tag{1}$$

where $F$ is the force applied to the cantilever (loading force), $\delta$ is the indentation depth, $\nu$ is the cellular Poisson's ratio (assumed to be 0.5 for incompressible biological material), and $2\phi$ is the tip angle (25–45°). Curve fitting was performed using the data analysis software Igor Pro (version 6.3.7.2; WaveMetrics, Portland, OR) along with the software MFP-3D (version 14.23.153; Asylum Research, Santa Barbara, CA).

To quantify membrane stiffness, we analyzed the approach force curves from the point at which the cantilever initially touched the cell surface to a point where the cantilever made an indentation to a depth of ~5 nm on the surface (corresponding to the approximate thickness of the membrane bilayer) (23), as shown in the section of the representative traces in Fig. 1 *A*. For the stiffness of the deeper cytoskeleton, on the other hand, the entire approach force curve with the indentation to the depth of 500 nm or ~10–15% of the total cell height was fitted to the Hertz model, as illustrated in the representative traces for cells in isotonic and hypotonic solutions in Fig. 1 *B*. An inset to Fig. 1 schematically shows the different regions. Both portions of the curves were fitted to the Hertz model to extract values of $E$. Because the measurement is done by the AFM probe

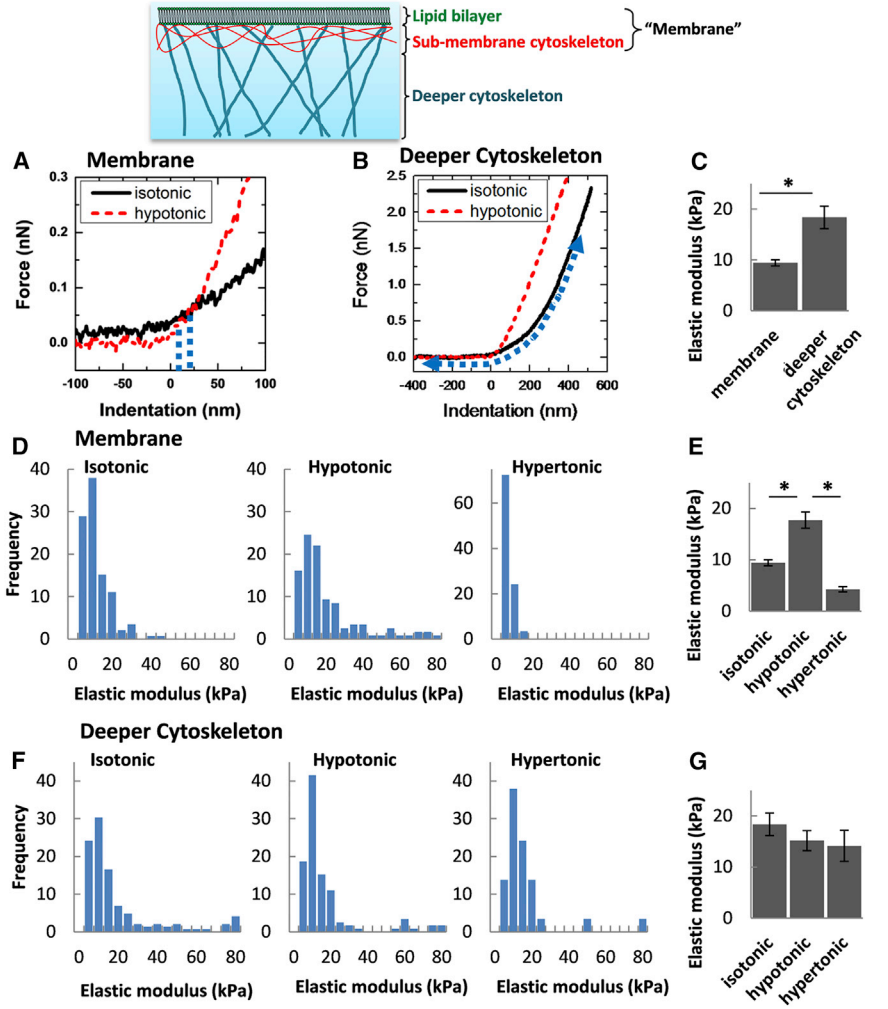


FIGURE 1 Differential effects of isotonic and hypotonic solutions on membrane region and deeper cytoskeleton elastic moduli. (*Inset*) schematic depicting a cell membrane segment illustrating the positions of the membrane (composed of the lipid bilayer/submembrane cytoskeleton complex) and the deeper cytoskeleton. (*A*) Sections of representative traces of AFM approach force curves for cells exposed to osmotic challenge, with vertical dashed lines demarcating the section fitted to obtain the membrane region elastic modulus. (*B*) Full representative traces of approach force curves, with a dashed curve indicating the region fitted to obtain elastic moduli of the deeper cytoskeleton. (*C*) Mean membrane and deeper cytoskeleton elastic moduli of cells exposed to isotonic solution. (*D*) Histograms of elastic moduli measured in the membrane region of endothelial cells exposed to isotonic (*left*), hypotonic (*center*), and hypertonic (*right*) solutions. (*E*) Mean membrane region elastic moduli of cells exposed to the conditions described above. (*F*) Histograms of elastic moduli measured in the deeper cytoskeleton of cells exposed to isotonic, hypotonic, and hypertonic solutions. (*G*) Mean deeper cytoskeletal elastic moduli of cells exposed to the same experimental conditions ($n$ = 15–60 cells; $p < 0.05$). Data was obtained immediately after the onset of osmotic challenge and continued for 25 min. To see this figure in color, go online.

approaching cells from above and measuring the stiffness of the apical membrane, the extracellular matrix at the cell-substrate interface does not contribute to this measurement.

One limitation of this method is that, although cells are heterogeneous, the Hertz model assumes sample homogeneity. However, this model is the most common method to estimate cellular elastic moduli from AFM indentation experiments and used in numerous studies (24–26). Therefore, whereas other models have been developed to estimate elastic moduli from AFM data, we chose to use the Hertz model to obtain parameters consistent with values obtained in other studies. Another limitation of the method is that under different experimental conditions, the lattice spacing of the deep cytoskeleton may change, affecting how deeply the AFM cantilever tip can penetrate at a given applied force. Although this change in lattice spacing could potentially affect the measured stiffness of the deep cytoskeleton, we believe that our estimates of membrane stiffness are unaffected because we obtain these values at a constant indentation depth of 5 nm, regardless of experimental condition.

To study the effect of hypotonic challenge on endothelial membrane tension, we determined the force of membrane tether formation using nonfunctionalized AFM cantilever tips. Multiple force curves were obtained per cell by repeatedly indenting two distinct regions on each cell. As the AFM probe retracted from the cell, the surface of the membrane occasionally adhered to the silicon nitride cantilever tip and was pulled up to form a membrane nanotube (tether). In these cases, as the probe was retracted further away from the cell, the membrane tether ruptured from the cantilever tip, causing a sudden jump in the force recorded on the force/distance retraction curve, thus providing a way to quantify the force required to form a cell membrane tether. Mean tether force values were obtained by analysis of at least ten retraction force curves at both locations probed on each cell. Only curves that exhibited an adhesion event between the cantilever tip and the cell membrane were selected for analysis. The radii of the tethers were not measured because in AFM experiments, the direction at which tethers are pulled is the same as the optical axis of the microscope and, therefore, tethers cannot be directly visualized. Formation of the tethers is determined by the sudden change in force with distance as the tethers detach from the cantilever tip.

## Data analysis

Elastic modulus ($E$) values obtained from fitting experimental force curves to the Hertz model (Eq. 1) are presented for each experimental condition both as histograms (binned in increments of 5 kPa for both control and hypotonically challenged cells and 0.5 kPa for latrunculin-treated cells) and as mean ± SE from at least three independent experiments. A similar method is used to present tether force data. For analysis of the effects of time on $E$ and tether force, data is averaged separately for each cell and plotted on one graph as a function of time, aggregated for all independent experiments. Statistical analysis of the data is performed using standard two-sample Student's $t$-tests and assuming unequal variances of the data

sets. Two-tailed distributions have been assumed to obtain statistical significance and the confidence interval is set to at least a 95% level ($p < 0.05$).

## RESULTS

### Distinct effects of osmotic challenge on the membrane and deeper cytoskeleton stiffness

We studied the impact of osmotic stress on the stiffness of HAECs measured by AFM nanoindentation for confluent HAECs exposed to isotonic and 20% hypotonic or hypertonic osmotic gradient conditions. The schematic inset in Fig. 1 illustrates the two regions of interest, a membrane bilayer with the underlying submembrane cytoskeleton (membrane) and the deeper cytoskeleton. The regions are probed by AFM to obtain estimates of the membrane elastic modulus (analysis of the indentation to a depth of 5 nm; Fig. 1 *A*) and deeper cytoskeleton (analysis of the indentation to a depth of 500 nm; Fig. 1 *B*). Notably, the stiffness of the deeper cytoskeleton is double that of the membrane region, indicating that the overall cellular stiffness is higher than that of the membrane-cytoskeleton envelope (Fig. 1 *C*).

Exposure of HAECs to a hypotonic solution causes a significant increase in membrane stiffness (Fig. 1, *D* and *E*). This is apparent in Fig. 1 *D* from the right-tailing and spreading observed in the distribution of membrane elastic moduli ($E$) measured in cells exposed to the hypotonic solution, as compared to cells in isotonic medium, and from an increase in the mean value of the membrane $E$ (Fig. 1 *E*). Conversely, exposure of HAECs to a hypertonic solution causes a significant decrease in membrane elastic moduli (Fig. 1, *D* and *E*). In contrast, our analysis of the full approach curves (shown in Fig. 1 *B*), yielding elastic moduli of the deeper cytoskeleton, shows no significant change under either hypotonic or hypertonic conditions (Fig. 1, *F* and *G*).

Numerous studies have shown that challenging cells with hypotonic gradients results in a transient increase in cell volume followed by a recovery phase called "regulatory volume decrease" (RVD) (reviewed by (17,27)). It is important, therefore, to analyze in more detail, the time dependence of the changes in endothelial elastic moduli after osmotic challenge. Using resistance measurements in a microfluidic chamber described in our earlier study (28), we show that aortic endothelial cells undergo a typical RVD process with a recovery observed within ~15–20 min after the onset of osmotic challenge. A representative RVD trace from an endothelial cell is shown as an inset in Fig. 2. From Fig. 2 *A*, we can clearly see that the membrane $E$ values for cells in isotonic solution remain constant over time and average 10.4 ± 1.2 kPa, whereas, when the solution is switched to a hypotonic one, the membrane $E$ begins to increase, as evidenced by the scattering of $E$ values over 25 min in Fig. 2 *A*. Taking mean values of membrane $E$ every 5 min for the duration of the experiment in Fig. 2 *B* (and averaging all 25 min of values for isotonic solution for the first data point at time 1 min), we observe an initial increase in stiffness with time, followed by a plateau and slight decrease.

### Disruption of F-actin enhances membrane-cytoskeleton stiffening

It is well established that cell stiffness depends primarily on the cytoskeleton and that disruption of the F-actin network results in a significant decrease in the cellular elastic modulus (29). It is also possible that osmotic flow of water and solutes into the cell could cause stiffening of the membrane region by increasing the hydrostatic pressure. To discriminate between these possibilities, cells were exposed to latrunculin A (lat-A), a toxin that prevents actin

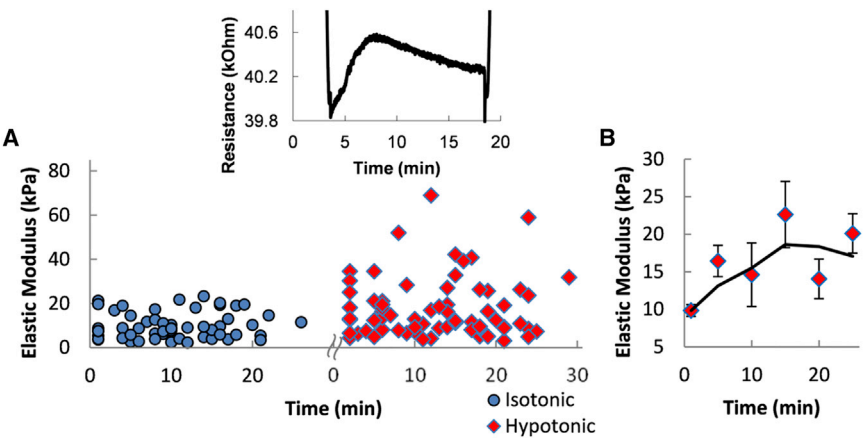


FIGURE 2 Time dependence of changes to elastic moduli by hypotonic challenge. (*Inset*) Representative trace of RVD response of aortic endothelial cells challenged with an osmotic gradient. (*A*) Time dependence of membrane elastic moduli changes for cells exposed first to isotonic and then hypotonic solutions. (*B*) Time-averaged membrane region elastic moduli, with the first data point being an average for all cells in isotonic media, and subsequent data points representing cells in hypotonic medium averaged every 5 min. The line shows the moving average of every two points. Note that RVD measurements are performed in a microfluidic chamber under shear stress, as described in our earlier studies (28), and AFM measurements are performed in an open chamber under static conditions. The difference between the two sets of conditions for RVD and AFM experiments may account for the differences in the time-courses of volume change and of membrane elastic modulus. To see this figure in color, go online.

polymerization, resulting in a collapse of the F-actin network (30). In our experiments, cells were exposed to 1 $\mu$M lat-A for 10 min under isotonic conditions and then the medium was changed to a hypotonic solution. As expected, exposure to lat-A resulted in a dramatic change in endothelial morphology, with cells becoming round and losing cell-cell contacts, indicating the collapse of the F-actin network. Also, as expected, exposure to lat-A resulted in a significant decrease in the elastic moduli of both the membrane region (1.3 $\pm$ 0.3 vs. 10.4 $\pm$ 1.2 kPa for cells exposed to lat-A versus control cells in isotonic conditions, respectively) and cytoskeleton (3.5 $\pm$ 0.6 vs. 20.0 $\pm$ 4.2 kPa for lat-A treated versus control cells in isotonic solution, respectively). This shift is also apparent from a decrease in the initial slopes of the approach force curves after the point of cell indentation by the AFM cantilever, shown in representative traces in Figs. 3 *A* and 4 *A* for cells in both isotonic and hypotonic solutions treated with lat-A, as compared to similar traces for untreated cells in Fig. 1, *A* and *B*.

However, despite the loss of F-actin network, hypotonically induced stiffening of the membrane region of the cells persisted (Fig. 3). Specifically, from the representative traces for lat-A treated cells, it is immediately clear that the cells exposed to hypotonic solutions are stiffer than those in isotonic medium (see the *shift in slopes* in Fig. 3 *A*). This effect is quantitatively demonstrated in Fig. 3 *B* by showing both right shifting and spreading of the membrane $E$ distribution for cells in hypotonic solution as compared to cells in isotonic medium. There is also a statistically significant increase in the mean value of $E$ in cells challenged with a hypotonic solution (Fig. 3 *C*). Furthermore, we show here that depolymerization of F-actin enhances the stiffening effect of the membrane region by hypotonic solution (hypotonic to isotonic $E$ ratio of 2.6 $\pm$ 0.2 for lat-A treated cells versus 1.8 $\pm$ 0.2 for control cells, $p < 0.05$), suggesting that the presence of the intact cytoskeleton dampens the stiffening effect. Notably, there is also a significant change in the time-course of the stiffening effect: whereas in control, untreated cells the stiffening persisted over a range of at least 25 min, after lat-A treatment, the stiffening becomes biphasic (Fig. 3 *D*). First, exposure to the hypotonic solution results in a transient (2.7 $\pm$ 0.3)-fold increase in the mean membrane $E$ within the first 6 min after the osmotic challenge (from 1.3 $\pm$ 0.1 kPa for isotonic to 3.5 $\pm$ 0.3 kPa for hypotonic solution, $p < 0.01$), and then it stabilizes to a mean value of 2.5 $\pm$ 0.2 kPa in hypotonic solution. The biphasic change in the elastic modulus suggests that RVD in these cells is facilitated by the disruption of F-actin. Although this prediction cannot be tested experimentally using our methodology because lat-A treated cells lose their adhesion to the substrate, our earlier studies showed that disruption of F-actin facilitates activation of volume-regulated anion channels (14), which indeed would be expected to facilitate RVD.

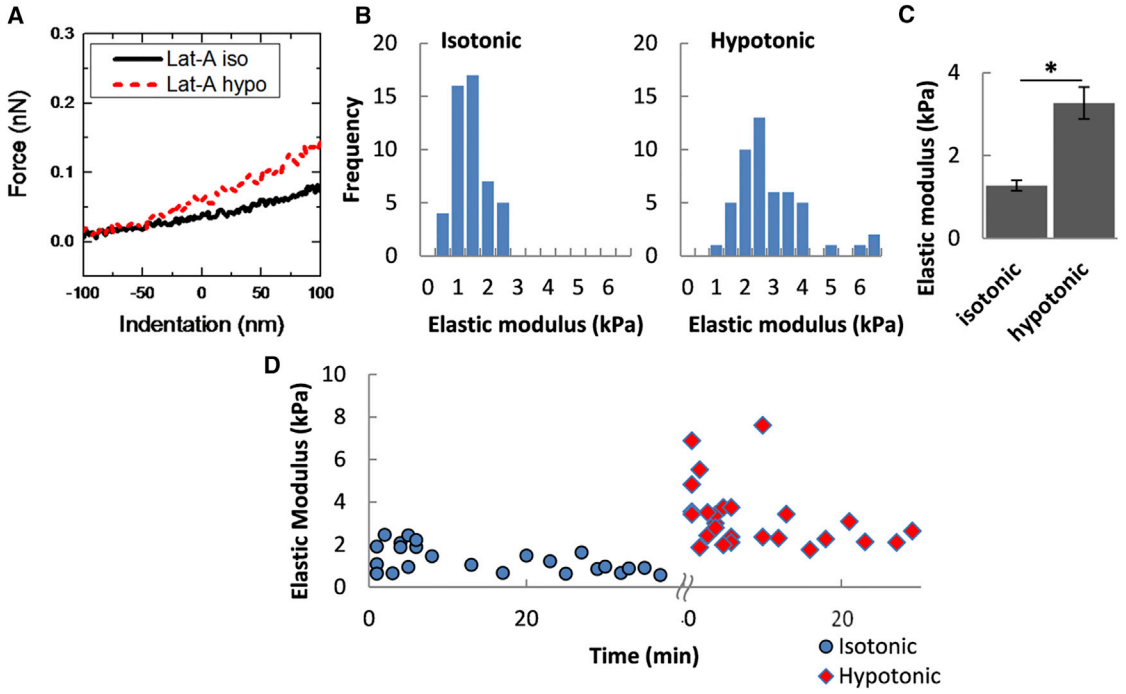


FIGURE 3 Dependence of membrane elastic moduli on F-actin disruption. (*A*) Sections of representative traces of approach force curves for lat-A-treated cells (1 $\mu$M for 10 min), exposed to an osmotic challenge. (*B*) Histograms of membrane elastic moduli of lat-A-treated cells exposed to isotonic (*left*) and hypotonic (*right*) solutions. (*C*) Mean membrane elastic moduli of lat-A-treated cells exposed to isotonic and hypotonic solutions. (*D*) Time dependence of membrane elastic moduli changes for lat-A-treated cells exposed first to isotonic and then hypotonic solutions ($n$ = 15–60 cells; $p < 0.05$). To see this figure in color, go online.

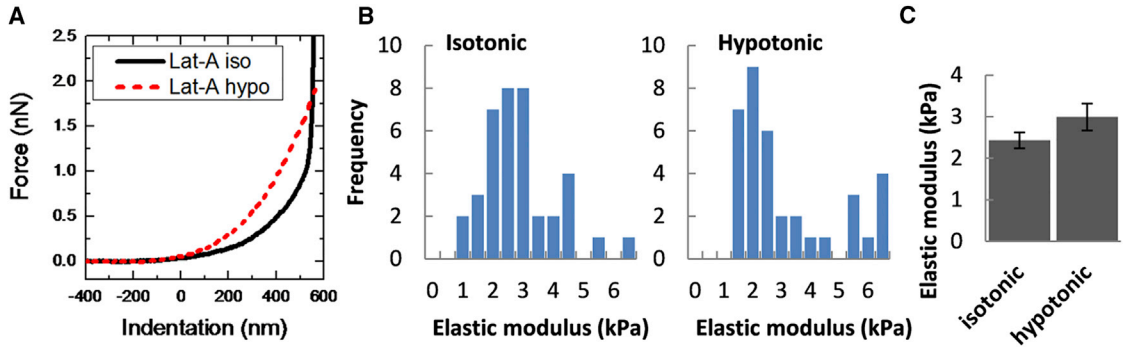


FIGURE 4 Dependence of deeper cytoskeletal elastic moduli on F-actin disruption. (*A*) Full representative traces of approach force curves for lat-A-treated cells (1 $\mu$M for 10 min), exposed to an osmotic challenge. (*B*) Histograms of elastic moduli measured in the deeper cytoskeleton of lat-A treated cells exposed to isotonic (*left*) and hypotonic (*right*) solutions. (*C*) Mean deeper cytoskeletal elastic moduli of lat-A treated cells exposed to isotonic and hypotonic solutions. To see this figure in color, go online.

In contrast to this increase in membrane $E$, no significant change was observed in the deeper cytoskeleton stiffness in lat-A treated cells upon osmotic challenge (Fig. 4). Taken together, these observations demonstrate that the stiffness of the membrane region is more sensitive to changes in osmotic pressure than the stiffness of the cytoskeleton.

### Osmotic challenge does not increase membrane tether force

Formation of membrane tethers is used to estimate cell membrane tension by optical tweezers (3,31) or atomic force microscopy (32,33). The tether force obtained from these measurements is composed of 1) the lipid bilayer in-plane tension, 2) the membrane resistance to tether formation (bending stiffness), and 3) the membrane-cortical cytoskeleton adhesion energy (34). Therefore, tether forces are also able to provide an estimate of the strength of adhesion between the membrane and the underlying cortical cytoskeleton.

Our analyses of the retraction force curves that exhibit membrane tethers produced distributions of tether forces, shown in Fig. 5 *B*, where we observe similar distributions for cells residing in both isotonic and hypotonic solutions. Averaging these distributions indicates that exposure of HAECs to hypotonic challenge does not cause a significant change in the overall force of membrane tether formation (Fig. 5 *C*). Furthermore, we also measured the tether forces after disrupting F-actin with lat-A to estimate the contribution of membrane-cytoskeleton adhesion to tether formation. These data show that, as expected (30), the tether forces in both isotonic and hypotonic conditions are significantly reduced, but there is no difference between the two conditions (Fig. 5 *C*). These observations suggest that hypotonic challenge has no significant effect on the membrane-cytoskeleton adhesion in HAECs. Notably, the tether force is also constant with time throughout the experimental period for cells in both isotonic and hypotonic solutions (Fig. 5, *D* and *E*). This indicates that cell swelling due to osmotic challenge does not have an effect on the formation of membrane tethers by AFM nanoindentation.

## DISCUSSION

The impact of cell swelling on cellular biomechanics and particularly on membrane tension has been a major question in the field of cell volume regulation. The general expectation is that, as cells swell, membrane tension should increase; however, there is little direct evidence to support this notion. It is also expected that upon swelling, the elastic modulus of the cells should decrease, representing cell softening, because earlier studies showed that cell swelling results in the disruption and reorganization of the cortical cytoskeleton (14–21). In this study, we analyze the impact of cell swelling on the biomechanical properties of human aortic endothelial cells by simultaneous measurements of endothelial elastic moduli and the force required for the formation of membrane tethers. Moreover, our analysis discriminates between the elastic modulus of the membrane/cytoskeletal complex (i.e., membrane) and the general elastic modulus of the cell, which represents the resistance to deformation of the deeper cytoskeleton throughout the whole cell. Our main findings are: 1) cell swelling results in a significant increase in the membrane elastic modulus, indicating that it becomes stiffer, an effect that is enhanced, not abrogated, by the disruption of F-actin; 2) there is no significant change in the general elastic modulus of swollen cells; and 3) no effect is observed on the force needed for membrane tether formation, suggesting that membrane tension of HAECs is not affected by cell swelling. We propose that an increase in the membrane elastic modulus is the result of increased hydrostatic pressure within the cell due to the influx of water into the cell resulting from the osmotic gradient.

It is known that the plasma membrane is tightly associated with the submembrane cytoskeleton layer, creating a membrane/cytoskeleton complex. It is also known that the submembrane cytoskeleton is the major determinant of the

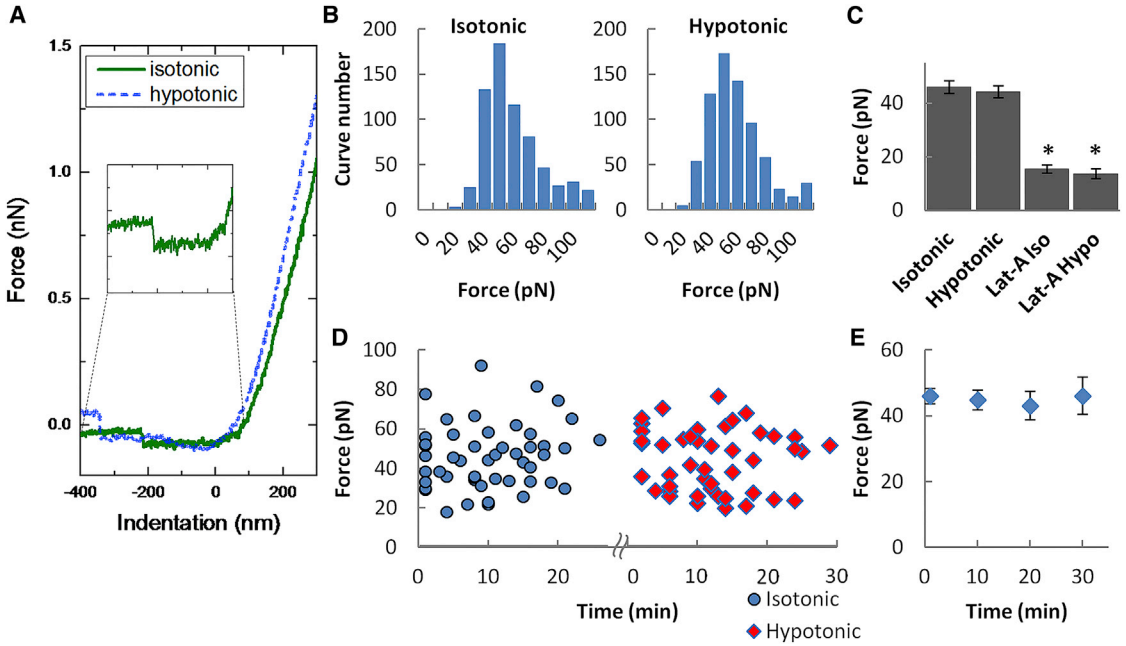


FIGURE 5 Effect of osmotic challenge on the force of membrane tether formation. (*A*) Representative traces of AFM retraction force curves for cells exposed to an osmotic challenge with an inset of a representative force discontinuity (used to obtain the tether force). (*B*) Histograms of membrane tether forces measured in cells exposed to isotonic (*left*) and hypotonic (*right*) solutions. (*C*) Mean membrane tether forces of cells exposed to isotonic and hypotonic solutions with and without exposure to lat-A (1 $\mu$M for 10 min). (*D*) Time dependence of membrane tether force measurements for cells exposed first to isotonic and then hypotonic solutions. (*E*) Time-averaged tether force measurements, with the first data point being an average for all cells in isotonic media, and subsequent data points representing cells in hypotonic medium averaged every 10 min (*asterisks* denote statistically significant difference ($n$ = 15–60 cells; $p < 0.05$) between lat-A-treated and untreated cells). To see this figure in color, go online.

elastic properties of this complex, meaning that the elastic properties of the membrane depend primarily on the mechanical properties of the submembrane cytoskeleton and not on the elastic properties of the lipid bilayer (35–39). Therefore, disruption of the submembrane cytoskeleton or its detachment from the membrane bilayer should decrease membrane elastic modulus. Our initial expectation, therefore, was that because cell swelling was shown previously to cause partial disruption of the cytoskeleton, it should cause a decrease in membrane elastic modulus. In this study, however, we show that a mild osmotic gradient of 20% results in a significant increase in elastic modulus of the membrane region in HAECs. It is important to note that, whereas many studies analyze the effects of cell swelling by subjecting the cells to osmotic gradients of 50% or more (3–6,40) including exposing the cells to distilled water (41,42), these strong gradients are very unlikely to be physiologically relevant because the osmolality of the plasma and extracellular fluids is tightly regulated. For example, even under extreme conditions of compulsive water drinking, we found that the osmolality of the plasma decreases ~10% (43). This study, therefore, focuses on a mild osmotic gradient that is closer to physiological challenges.

In terms of the mechanism for the observed hypotonically induced membrane stiffening, we considered two general mechanisms. One possibility is that, even though osmotic swelling has been shown to result in the dislocation of the cortical cytoskeleton (fodrin) from the endothelial membrane (18), it is possible that there are additional cytoskeletal changes that could result in membrane stiffening. An alternative possibility is that the stiffening is a result of an increased hydrostatic pressure that develops from osmotic influx into the cells. This increased pressure may cause the measured elastic modulus to increase. Indeed, Beyder and Sachs (44) showed that the application of hydrostatic pressure through a micropipette directly to the cell interior in a whole-cell patch configuration results in a decrease in membrane deformability, which indicates membrane stiffening. To discriminate between these possibilities, we tested whether depolymerization of F-actin, which causes a collapse of the cytoskeleton (18,32), abrogates the observed stiffening effect. As expected, we observed a dramatic decrease in the elastic modulus for cells treated with latrunculin A, indicating the collapse of the cytoskeleton and possibly the transfer of stress from deep cytoskeleton to the cortex. These data are also consistent with several studies from our lab and from other investigators showing that endothelial cells are contractile under control conditions, as measured both by traction force microscopy and in 3D collagen gels (45,46). Collapsing the F-actin network is expected to abrogate the contractile response. However, at the same time, we found that the depolymerization of F-actin did not abrogate, but actually enhanced, the increase in the membrane elastic modulus of the cells during osmotic

challenge. This observation strongly supports the hypothesis that it is an increase in hydrostatic pressure that is responsible for the observed stiffening effect. Notably, very little is currently known about the effects of intracellular hydrostatic pressure on cellular signaling mechanisms and further studies are needed to evaluate these effects. In terms of the effect of the hydrostatic pressure on membrane elastic modulus, we propose that it can be a direct result of physical pressure applied to the membrane from inside. Furthermore, our observation that the hypotonically induced stiffening of the membrane is enhanced after depolymerization of F-actin suggests that an increase in hydrostatic pressure is partially balanced by the cytoskeletal networks, possibly via a sponge effect, described below.

With regard to the elastic modulus of the deeper cytoskeleton of HAECs as a result of cell swelling, earlier studies showed mild softening in several cell types, including primary astrocytes and HEK cells (47) and stiffening in cortical neurons (48). One possibility is that cell softening can be a result of the perturbation of the cytoskeletal networks, which may include a mild depolymerization of F-actin and/or disruption of the cross-linking between the fibers (reviewed by Pedersen et al. (49)). An alternative possibility, proposed recently by Sachs and Sivaselvan (50), is that cell softening during cell swelling may be a result of a sponge effect. This hypothesis is based on previous studies describing the cytoplasm as a poroelastic structure similar to a soft, fluid-filled sponge, due to the cross-linked filaments of the deeper cytoskeleton (51). We observed no significant changes in the elastic moduli of the deeper cytoskeleton of aortic endothelial cells under either hypotonic or hypertonic conditions used in our study, which is consistent with an earlier study showing that osmotic challenge affects the submembrane F-actin but not that of the deeper cytoskeleton (21).

Analysis of membrane tethers provides an additional independent method to characterize membrane biomechanics. As tethers are pulled from cell membranes, the membrane exerts a retractile force on the tether as the constituent lipids of the tether are drawn back toward the membrane, creating tension in the plane of the membrane (52). This in-plane tension, along with the adhesion between the membrane and cortical cytoskeleton, are combined into a single term for membrane tension ($T_m$) because the two parameters are inextricable from one another (9). The force required to pull a tether (tether force, $F$) is a function of $T_m$ and can be defined as the simplified relationship in Eq. 2, previously proposed by Sheetz and Dai (52):

$$F = 2\pi R T_m + \pi \frac{B}{R}, \tag{2}$$

where $R$ is the tether radius and $B$ is the intrinsic membrane bending stiffness, which resists the formation of tethers due to the large changes in membrane curvature required to form these nanotubes (53). The membrane bending stiffness can be estimated using the static tether force (Eq. 3) (34,54):

$$B = \frac{FR}{2\pi}, \tag{3}$$

where the values of $F$ and $R$ are measured experimentally. Previous studies estimated $B$ values for lipid bilayers and for the cellular membranes of red blood cells and neutrophils to be $\sim 10^{-19}$ N·m (54–56). Estimating membrane bending stiffness from our measurements of tether force yields values in a similar range; the tether forces measured in our experiments are in the range of ~40 pN, and although we cannot measure the radii of the tethers, as discussed in the Materials and Methods, assuming the average tether radii of 50–100 nm, similar to those reported in previous studies (57), yields $B$ values of $\sim 3 \times 10^{-19}$–$6 \times 10^{-19}$ N·m. The relationship between membrane bending moduli estimated from membrane tethers and elastic moduli estimated from the indentation force curves, however, is complicated, presumably because of the different nature of the measurements, which are sensitive to distinct components of the membrane. Furthermore, measuring membrane tether forces with and without disruption of the cytoskeleton allows estimation of the contribution of the adhesion energy between the membrane and the cytoskeleton. If we assume that lat-A treatment results in the loss of membrane/cytoskeleton adhesion, then the adhesion energy ($\gamma$) can be estimated from

$$\gamma = \frac{F^2 - F_{\text{lat}}^2}{8B\pi^2}, \tag{4}$$

where $F_{\text{lat}}$ is the tether force in the absence of membrane/cytoskeleton adhesion. Because we show here that there is no difference in either $F$ or $F_{\text{lat}}$ values between the isotonic and hypotonic conditions, we can conclude that mild hypotonic swelling does not change membrane/cytoskeleton adhesion energy.

These observations are also consistent with a previous study by Sinha et al. (8), who found that hypotonic swelling did not increase membrane tension in endothelial cells unless they were devoid of caveolin. This observation was interpreted as evidence that swelling of endothelial cells resulted from unfolding of membrane reservoirs, so that an increase in membrane tension was buffered by the presence of caveolae. Similarly, Raucher and Sheetz (4), Dai et al. (3,5), Groulx et al. (6), and Dai and Sheetz (9) showed that only very small increases in membrane tension were observed in neurons, fibroblasts, leukemia, and lung carcinoma cells, which was also interpreted to indicate the existence of membrane folds and lipid reservoirs (e.g., blebs, microvilli, caveolae) that control and buffer membrane tension (58). It is also interesting to note that the range of tether forces that we measured in this study in HAECs (>40 pN) is relatively high compared to previous studies

(20–30 pN) (32), which was proposed earlier to reflect strong membrane/cytoskeletal adhesion (52). Our observations that neither tether force nor estimated adhesion energy increase upon swelling, suggest that the membrane unfolds together with the underlying cytoskeleton. Moreover, it is important to note that, whereas it may seem counterintuitive that membrane unfolding does not require detachment from the cytoskeleton, this is fully consistent with earlier studies by Akinlaja and Sachs (59), who pointed out that membrane bilayer lipids may flow freely through the cytoskeleton when external pressure is applied. Interestingly, Sachs and colleagues also showed that exposing different types of cells to hypotonic conditions result in a transient decrease with a subsequent increase in the cytoskeletal tension, as assessed by FRET-based assay of $\alpha$-actinin (42), a major actin-binding protein (60), or actin (41). Thus, it appears that changes in cytoskeletal tension do not necessarily correspond to changes in membrane tension, as assayed by membrane tethers.

In summary, in this study, we show that hypotonic swelling of endothelial cells results in significant stiffening of the membrane, which we suggest to be attributed to an increase in hydrostatic pressure. Importantly, no change is observed in membrane tether force/membrane tension upon osmotic swelling. The implication of these findings is that activation of swelling-sensitive ion channels and signaling pathways might be initiated by an increase in cellular hydrostatic pressure rather than increased membrane tension. This notion would also be consistent with our earlier studies showing that F-actin disruption enhances activation of volume-sensitive anion channels (14). It is also important to note that swelling-sensitive ion channels are known to be activated by a decrease in cytoplasmic ionic strength that results from water influx into the cells (61–64). Because both hydrostatic pressure and a change in ionic strength are expected to be affected by increased swelling after disruption of the cortical cytoskeleton, it is difficult to discriminate between the contributions of these mechanisms to the activation of the channels. Moreover, our conclusion that mild hypotonic swelling does not necessarily result in increased membrane tension has important implications on membrane biomechanics because it indicates that hypotonic swelling may not be an appropriate approach to determine the role of membrane tension in different mechanosensitive phenomena.

## AUTHOR CONTRIBUTIONS

M.A.A.A. and I.L. wrote the manuscript and designed research. M.A.A.A. performed research. E.L., T.T., and J.L. contributed analytic tools. M.A.A.A. and I.L analyzed data.

## ACKNOWLEDGMENTS

This study was supported by National Institutes of Health (NIH) grants T32 HL-82547 (to M.A.A.A.), HL-083298, and HL-073965 (to I.L.).

## REFERENCES

1. Okada, Y., E. Maeno, …, S. Morishima. 2001. Receptor-mediated control of regulatory volume decrease (RVD) and apoptotic volume decrease (AVD). *J. Physiol.* 532:3–16.
2. Hoffmann, E. K., and P. B. Dunham. 1995. Membrane mechanisms and intracellular signalling in cell volume regulation. *Int. Rev. Cytol.* 161:173–262.
3. Dai, J., M. P. Sheetz, …, C. E. Morris. 1998. Membrane tension in swelling and shrinking molluscan neurons. *J. Neurosci.* 18:6681–6692.
4. Raucher, D., and M. P. Sheetz. 1999. Characteristics of a membrane reservoir buffering membrane tension. *Biophys. J.* 77:1992–2002.
5. Dai, J., H. P. Ting-Beall, and M. P. Sheetz. 1997. The secretion-coupled endocytosis correlates with membrane tension changes in RBL 2H3 cells. *J. Gen. Physiol.* 110:1–10.
6. Groulx, N., F. Boudreault, …, R. Grygorczyk. 2006. Membrane reserves and hypotonic cell swelling. *J. Membr. Biol.* 214:43–56.
7. Vlahakis, N. E., and R. D. Hubmayr. 2000. Invited review: plasma membrane stress failure in alveolar epithelial cells. *J. Appl. Physiol.* 89:2490–2496, discussion 2497.
8. Sinha, B., D. Köster, …, P. Nassoy. 2011. Cells respond to mechanical stress by rapid disassembly of caveolae. *Cell.* 144:402–413.
9. Dai, J., and M. P. Sheetz. 1999. Membrane tether formation from blebbing cells. *Biophys. J.* 77:3363–3370.
10. Sheetz, M. P. 2001. Cell control by membrane-cytoskeleton adhesion. *Nat. Rev. Mol. Cell Biol.* 2:392–396.
11. Kuznetsova, T. G., M. N. Starodubtseva, …, R. I. Zhdanov. 2007. Atomic force microscopy probing of cell elasticity. *Micron.* 38: 824–833.
12. Fletcher, D. A., and R. D. Mullins. 2010. Cell mechanics and the cytoskeleton. *Nature.* 463:485–492.
13. Wagner, B., R. Tharmann, …, A. R. Bausch. 2006. Cytoskeletal polymer networks: the molecular structure of cross-linkers determines macroscopic properties. *Proc. Natl. Acad. Sci. USA.* 103:13974–13978.
14. Levitan, I., C. Almonte, …, S. S. Garber. 1995. Modulation of a volume-regulated chloride current by F-actin. *J. Membr. Biol.* 147: 283–294.
15. Jorgensen, N. K., S. F. Pedersen, …, S.-P. Olesen. 2003. Cell swelling activates cloned $Ca^{2+}$-activated $K^+$ channels: a role for the F-actin cytoskeleton. *Biochim. Biophys. Acta.* 1615:115–125.
16. Lambert, I. H., E. K. Hoffmann, and S. F. Pedersen. 2008. Cell volume regulation: physiology and pathophysiology. *Acta Physiol. (Oxf.).* 194:255–282.
17. Hoffmann, E. K., I. H. Lambert, and S. F. Pedersen. 2009. Physiology of cell volume regulation in vertebrates. *Physiol. Rev.* 89:193–277.
18. Sun, A. C., and I. Levitan. 2003. Osmotic stress alters the intracellular distribution of non-erythroidal spectrin (fodrin) in bovine aortic endothelial cells. *J. Membr. Biol.* 192:9–17.
19. Pasantes-Morales, H., V. Cardin, and K. Tuz. 2000. Signaling events during swelling and regulatory volume decrease. *Neurochem. Res.* 25:1301–1314.
20. Hoffmann, E. K. 2000. Intracellular signalling involved in volume regulatory decrease. *Cell. Physiol. Biochem.* 10:273–288.
21. Pedersen, S. F., J. W. Mills, and E. K. Hoffmann. 1999. Role of the F-actin cytoskeleton in the RVD and RVI processes in Ehrlich ascites tumor cells. *Exp. Cell Res.* 252:63–74.
22. Lin, D. C., E. K. Dimitriadis, and F. Horkay. 2007. Robust strategies for automated AFM force curve analysis—I. Non-adhesive indentation of soft, inhomogeneous materials. *J. Biomech. Eng.* 129:430–440.
23. Edidin, M. 2003. Lipids on the frontier: a century of cell-membrane bilayers. *Nat. Rev. Mol. Cell Biol.* 4:414–418.
24. Schillers, H., C. Rianna, …, M. Radmacher. 2017. Standardized nanomechanical atomic force microscopy procedure (SNAP) for measuring soft and biological samples. *Sci. Rep.* 7:5117.

25. Haase, K., and A. E. Pelling. 2015. Investigating cell mechanics with atomic force microscopy. *J. R. Soc. Interface.* 12:20140970.
26. Thomas, G., N. A. Burnham, …, Q. Wen. 2013. Measuring the mechanical properties of living cells using atomic force microscopy. *J. Vis. Exp.* https://doi.org/10.3791/50497.
27. Lang, F., G. L. Busch, …, D. Häussinger. 1998. Functional significance of cell volume regulatory mechanisms. *Physiol. Rev.* 78:247–306.
28. Kowalsky, G. B., D. Beam, …, I. Levitan. 2011. Cholesterol depletion facilitates recovery from hypotonic cell swelling in CHO cells. *Cell. Physiol. Biochem.* 28:1247–1254.
29. Byfield, F. J., H. Aranda-Espinoza, …, I. Levitan. 2004. Cholesterol depletion increases membrane stiffness of aortic endothelial cells. *Biophys. J.* 87:3336–3343.
30. Spector, I., N. R. Shochet, …, Y. Kashman. 1989. Latrunculins—novel marine macrolides that disrupt microfilament organization and affect cell growth: I. Comparison with cytochalasin D. *Cell Motil. Cytoskeleton.* 13:127–144.
31. Lieber, A. D., S. Yehudai-Resheff, …, K. Keren. 2013. Membrane tension in rapidly moving cells is determined by cytoskeletal forces. *Curr. Biol.* 23:1409–1417.
32. Sun, M., N. Northup, …, G. Forgacs. 2007. The effect of cellular cholesterol on membrane-cytoskeleton adhesion. *J. Cell Sci.* 120: 2223–2231.
33. Diz-Muñoz, A., M. Krieg, …, C.-P. Heisenberg. 2010. Control of directed cell migration in vivo by membrane-to-cortex attachment. *PLoS Biol.* 8:e1000544.
34. Diz-Muñoz, A., D. A. Fletcher, and O. D. Weiner. 2013. Use the force: membrane tension as an organizer of cell shape and motility. *Trends Cell Biol.* 23:47–53.
35. Sato, M., D. P. Theret, …, R. M. Nerem. 1990. Application of the micropipette technique to the measurement of cultured porcine aortic endothelial cell viscoelastic properties. *J. Biomech. Eng.* 112:263–268.
36. Pourati, J., A. Maniotis, …, N. Wang. 1998. Is cytoskeletal tension a major determinant of cell deformability in adherent endothelial cells? *Am. J. Physiol.* 274:C1283–C1289.
37. Wu, H. W., T. Kuhn, and V. T. Moy. 1998. Mechanical properties of L929 cells measured by atomic force microscopy: effects of anticytoskeletal drugs and membrane crosslinking. *Scanning.* 20:389–397.
38. Rotsch, C., and M. Radmacher. 2000. Drug-induced changes of cytoskeletal structure and mechanics in fibroblasts: an atomic force microscopy study. *Biophys. J.* 78:520–535.
39. Zhang, G., M. Long, …, W.-Q. Yu. 2002. Mechanical properties of hepatocellular carcinoma cells. *World J. Gastroenterol.* 8:243–246.
40. Pietuch, A., B. R. Brückner, and A. Janshoff. 2013. Membrane tension homeostasis of epithelial cells through surface area regulation in response to osmotic stress. *Biochim. Biophys. Acta.* 1833:712–722.
41. Guo, J., Y. Wang, …, F. Meng. 2014. Actin stress in cell reprogramming. *Proc. Natl. Acad. Sci. USA.* 111:E5252–E5261.
42. Meng, F., and F. Sachs. 2011. Visualizing dynamic cytoplasmic forces with a compliance-matched FRET sensor. *J. Cell Sci.* 124:261–269.
43. Verghese, C., I. Levitan, …, R. C. Josiassen. 1997. Impaired lymphocyte volume regulation in schizophrenic patients with polydipsia-hyponatremia. *Biol. Psychiatry.* 42:733–736.
44. Beyder, A., and F. Sachs. 2009. Electromechanical coupling in the membranes of *Shaker*-transfected HEK cells. *Proc. Natl. Acad. Sci. USA.* 106:6626–6631.
45. Byfield, F. J., S. Tikku, …, I. Levitan. 2006. OxLDL increases endothelial stiffness, force generation, and network formation. *J. Lipid Res.* 47:715–723.
46. Norman, L. L., R. J. Oetama, …, H. Aranda-Espinoza. 2010. Modification of cellular cholesterol content affects traction force, adhesion and cell spreading. *Cell. Mol. Bioeng.* 3:151–162.
47. Spagnoli, C., A. Beyder, …, F. Sachs. 2008. Atomic force microscopy analysis of cell volume regulation. *Phys. Rev. E Stat. Nonlin. Soft Matter Phys.* 78:031916.
48. Zou, S., R. Chisholm, …, C. E. Morris. 2013. Force spectroscopy measurements show that cortical neurons exposed to excitotoxic agonists stiffen before showing evidence of bleb damage. *PLoS One.* 8:e73499.
49. Pedersen, S. F., E. K. Hoffmann, and J. W. Mills. 2001. The cytoskeleton and cell volume regulation. *Comp. Biochem. Physiol. A Mol. Integr. Physiol.* 130:385–399.
50. Sachs, F., and M. V. Sivaselvan. 2015. Cell volume control in three dimensions: water movement without solute movement. *J. gen. physiol.* 145:373–380.
51. Charras, G. T., T. J. Mitchison, and L. Mahadevan. 2009. Animal cell hydraulics. *J. Cell Sci.* 122:3233–3241.
52. Sheetz, M. P., and J. Dai. 1996. Modulation of membrane dynamics and cell motility by membrane tension. *Trends Cell Biol.* 6:85–89.
53. Dai, J., and M. P. Sheetz. 1995. Mechanical properties of neuronal growth cone membranes studied by tether formation with laser optical tweezers. *Biophys. J.* 68:988–996.
54. Hochmuth, F. M., J.-Y. Shao, …, M. P. Sheetz. 1996. Deformation and flow of membrane into tethers extracted from neuronal growth cones. *Biophys. J.* 70:358–369.
55. Bo, L., and R. E. Waugh. 1989. Determination of bilayer membrane bending stiffness by tether formation from giant, thin-walled vesicles. *Biophys. J.* 55:509–517.
56. Shao, J.-Y., and J. Xu. 2002. A modified micropipette aspiration technique and its application to tether formation from human neutrophils. *J. Biomech. Eng.* 124:388–396.
57. Pontes, B., Y. Ayala, …, H. M. Nussenzveig. 2013. Membrane elastic properties and cell function. *PLoS One.* 8:e67708.
58. Sens, P., and M. S. Turner. 2006. Budded membrane microdomains as tension regulators. *Phys. Rev. E Stat. Nonlin. Soft Matter Phys.* 73: 031918.
59. Akinlaja, J., and F. Sachs. 1998. The breakdown of cell membranes by electrical and mechanical stress. *Biophys. J.* 75:247–254.
60. Sjöblom, B., A. Salmazo, and K. Djinović-Carugo. 2008. $\alpha$-actinin structure and regulation. *Cell. Mol. Life Sci.* 65:2688–2701.
61. Nilius, B., J. Prenen, …, G. Droogmans. 1998. Activation of volume-regulated chloride currents by reduction of intracellular ionic strength in bovine endothelial cells. *J. Physiol.* 506:353–361.
62. Cannon, C. L., S. Basavappa, and K. Strange. 1998. Intracellular ionic strength regulates the volume sensitivity of a swelling-activated anion channel. *Am. J. Physiol.* 275:C416–C422.
63. Romanenko, V. G., G. H. Rothblat, and I. Levitan. 2004. Sensitivity of volume-regulated anion current to cholesterol structural analogues. *J. Gen. Physiol.* 123:77–87.
64. Syeda, R., Z. Qiu, …, A. Patapoutian. 2016. LRRC8 proteins form volume-regulated anion channels that sense ionic strength. *Cell.* 164:499–511.